ADVANCED MATERIALS
www.advmat.de

Colorless, Transparent, Robust, and Fast Scratch-Self-Healing Elastomers via a Phase-Locked Dynamic Bonds Design

Yue Lai, Xiao Kuang, Ping Zhu, Miaoming Huang, Xia Dong, and Dujin Wang*

Robust self-healing thermoplastic elastomers are expected to have repeated healing capability, remarkable mechanical properties, transparency, and superior toughness. The phase-locked design in this work provides excellent tensile mechanical properties and efficient healability at a moderate temperature due to the dynamic disulfide bonds embedded in the hard segments and mainly being locked in the viscoelastic hard microphase region. The self-healing elastomers exhibit a maximum tensile stress of 25 MPa and a fracture strain of over 1600%, which are quite prominent compared to previous reports. The nanoscale domains of the elastomer are smaller than the wavelength of visible light by microphase separation control resulting in colorless, nearly 100% transparency, and are as good as quartz glasses. The high dynamics of the phase-locked disulfide bonds renders a high healing efficiency of scratches on the surface within 60 s at 70 °C. The rapid scratch healing and complete transparency recovery of the elastomers provide new avenues in the highly transparent surface or protective films which finds potential applications for precision optical lenses, flexible display screens, and automobile or aircraft lighting finishes.

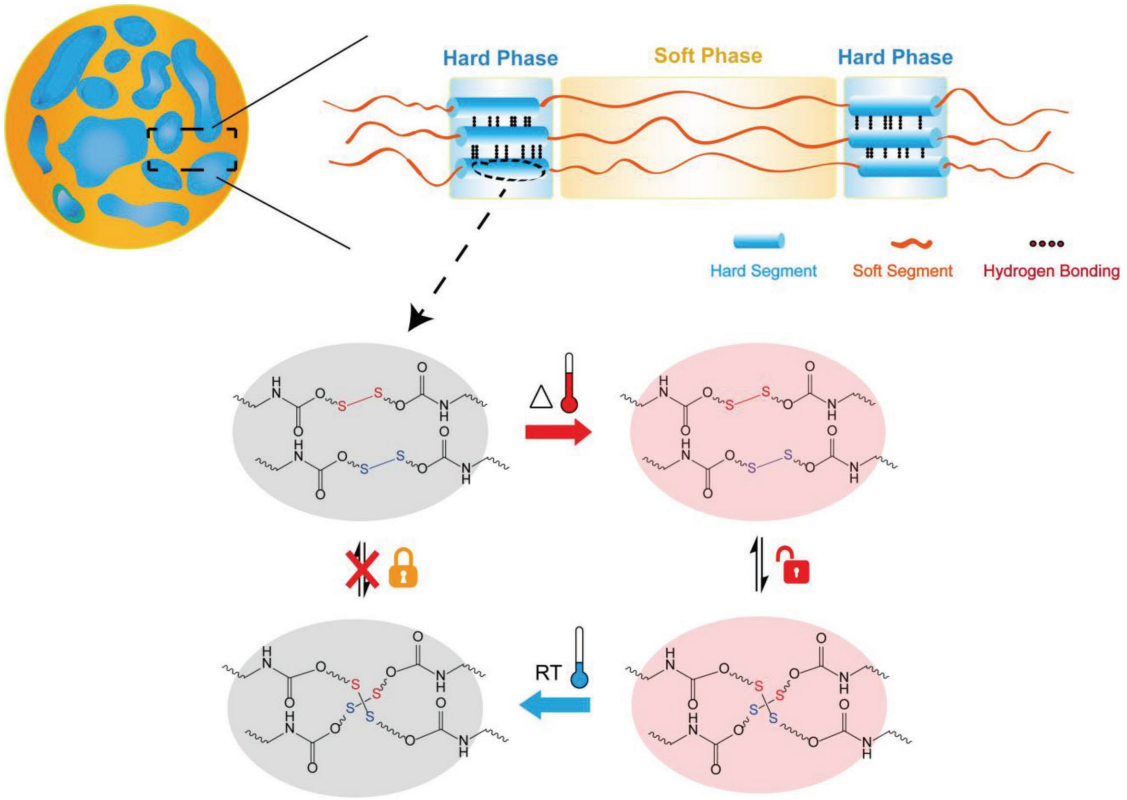
Motivated biologically, self-healing polymer systems capable of repairing cracks and restoring their original functions have been developed to improve the reliability and extending the service lifetime.[1] These systems have many potential applications, especially in the fields such as surface protection coatings,[2] biomedical materials,[3] and flexible electronics.[4] Various self-healing polymeric materials with different healing mechanisms, including extrinsic healing[5] and intrinsic healing,[6–8] have been fabricated. Recently, disulfide bond exchange reactions have attracted increasing attention due to their moderate reaction conditions and ability to respond to multiple stimuli.[9] To satisfy different applications, the self-healing glassy plastics, soft gels, and elastomers have been developed by incorporating disulfide linkages into polymeric materials.[4d,9a,b,10] The utilization of the aromatic disulfide compounds can yield rapid self-healing systems; however, this molecular design usually results in yellowish appearance as well as less transparency of the self-healing materials.[7b,f,11,12] In fact, the integration of excellent optical properties and mechanical properties for robust self-healing materials is a challenging task, which attracts great interest in both academia and industry.

Herein, from the perspective of molecular design, we propose a novel self-healing design strategy, "hard phase locking," to balance the mechanical robustness, the healing efficiency of self-healing elastomers, and the transparency. The self-healing polyurethane elastomers with disulfide bonds (PUDS) designed in this work exhibit colorless, superior transparency (close to the quartz glass), and maximum tensile stress of 25 MPa as well as a fracture strain over 1600%. The scratches on the surface of the elastomers can be rapidly healed within 60 s upon mild heating. Among various robust elastomers, thermoplastic polyurethane (TPU) is promising owing to its fine-tuned structure and microphase separation of soft segments and hard segments.[5d,13,14] An aliphatic disulfide–based self-healing TPU with distinct two-phase morphology combining high extensibility, excellent transparency, a widely tunable Young's modulus, and high healing efficiency at moderate temperatures was fabricated. As shown in **Scheme 1**, the self-healing TPU consists of stable and inert soft segments and active hard segments featuring dynamic aliphatic disulfides and strong hydrogen bonding interactions. Specifically, polytetramethylene ether glycol (PTMEG) with a moderate molecular weight (Mn = 1000) was used as the soft segment in the system, the hydrogenated 4,4′-methylenediphenyl diisocyanate (HMDI) and aliphatic disulfide bis(2-hydroxyethyl) disulfide (HEDS) were used as the hard segments. The high level of steric hindrance of the

Y. Lai, Dr. P. Zhu, Dr. M. Huang, Prof. X. Dong, Prof. D. Wang
CAS Key Laboratory of Engineering Plastics
CAS Research/Education Center for Excellence in Molecular Sciences
Institute of Chemistry
Chinese Academy of Sciences
Beijing 100190, P. R. China
E-mail: xiadong@iccas.ac.cn
Y. Lai, Prof. X. Dong, Prof. D. Wang
University of Chinese Academy of Sciences
Beijing 100049, P. R. China
Dr. X. Kuang
The George W. Woodruff School of Mechanical Engineering
Renewable Bioproduct Institute
Georgia Institute of Technology
Atlanta, GA 30332, USA
The ORCID identification number(s) for the author(s) of this article can be found under https://doi.org/10.1002/adma.201802556.

DOI: 10.1002/adma.201802556

 © 2018 WILEY-VCH Verlag GmbH & Co. KGaA, Weinheim



Scheme 1. The multiphase design and mechanism of tougher and more robust self-healing thermoplastic elastomers.

bulky alicyclic isocyanate results in the irregular packing of the molecular chains and thus effectively prevents crystallization. The moderate regularity and chain length of hard block generate relatively strong hydrogen bonding, which can enable strong microphase separation. In virtue of the microphase separation of TPU, the dynamic chemical bonds located in the hard segments are predominantly locked in the hard microphase domains. The dynamic bonds were immobilized in the microphase region below the glass transition temperature (T_g), which provides the elastomers with excellent tensile mechanical properties. More importantly, the locked bonds can be easily activated to be highly dynamic above the T_g and the elastomers possess effective self-healing and reprocessing ability.

The synthetic routes to the PUDS samples are shown in Figure S1 (Supporting Information). Several materials with different molar ratios of HMDI/HEDS (Table S1, Supporting Information) were synthesized. In addition, a blank control sample was obtained by using HDO (1,6-hexanediol) as a chain extender for the prepolymer instead of HEDS. The disulfide content of the samples was calculated using Equation S1 (Supporting Information). The disulfide content of the PUDS samples is shown in Table S2 (Supporting Information). The Raman spectra (Figure S3, Supporting Information), Fourier transform infrared spectra (FTIR) (Figure S4 and Table S3, Supporting Information), thermal gravimetric analysis (TGA) traces (Figure S5, Supporting Information), dynamic thermomechanical analysis (DMA) curves (Figure S6, Supporting Information), and the molecular weights (Table S2, Supporting Information) of the four samples are shown in the Supporting Information. Films for testing were prepared by casting the resins on Teflon plates, placing them in a fume cupboard for 24 h, and then removing the solvent at 80 °C for 24 h under vacuum. Finally, a series of transparent self-healing PUDSs were obtained, and no bubbles were observed inside the samples.

The mechanical properties of the PUDS samples were evaluated by tensile testing. Each of the sample shows a high tensile stress without compromising extension performance (**Figure 1**a). In particular, PUDS-8 has the highest maximum tensile stress of 25.0 MPa, which is very impressive among the reported self-healing materials.[5b–f,6c,d,7b,f,8a–c,9a,12,15–18] The increase of the disulfide content was accompanied by an increasing amount of hard segments, which act as physical crosslinks and a reinforcing element. As a result, the modulus and stiffness increase with the disulfide content. For example, Young's moduli of PUDS-8 and PUDS-9 are 34.56 and 56.05 MPa, respectively. Although the yield point is observed in the tensile curves of PUDS-8 and PUDS-9, these two samples also maintain a good ultimate tensile strain of approximately 1600%.

The microstructure of PUDS samples was investigated. Both the differential scanning calorimetry (DSC) data (Figure S7, Supporting Information) and the wide-angle X-ray scattering (WAXS) data (Figure S8, Supporting Information) indicate that the PUDS samples are amorphous without crystallinity. As the content of the hard segments increases, both the elctron density contrast between the two components and the period lengths of the system increase in small-angle X-ray scattering (SAXS) (Figure 1b), indicating more

© 2018 WILEY-VCH Verlag GmbH & Co. KGaA, Weinheim

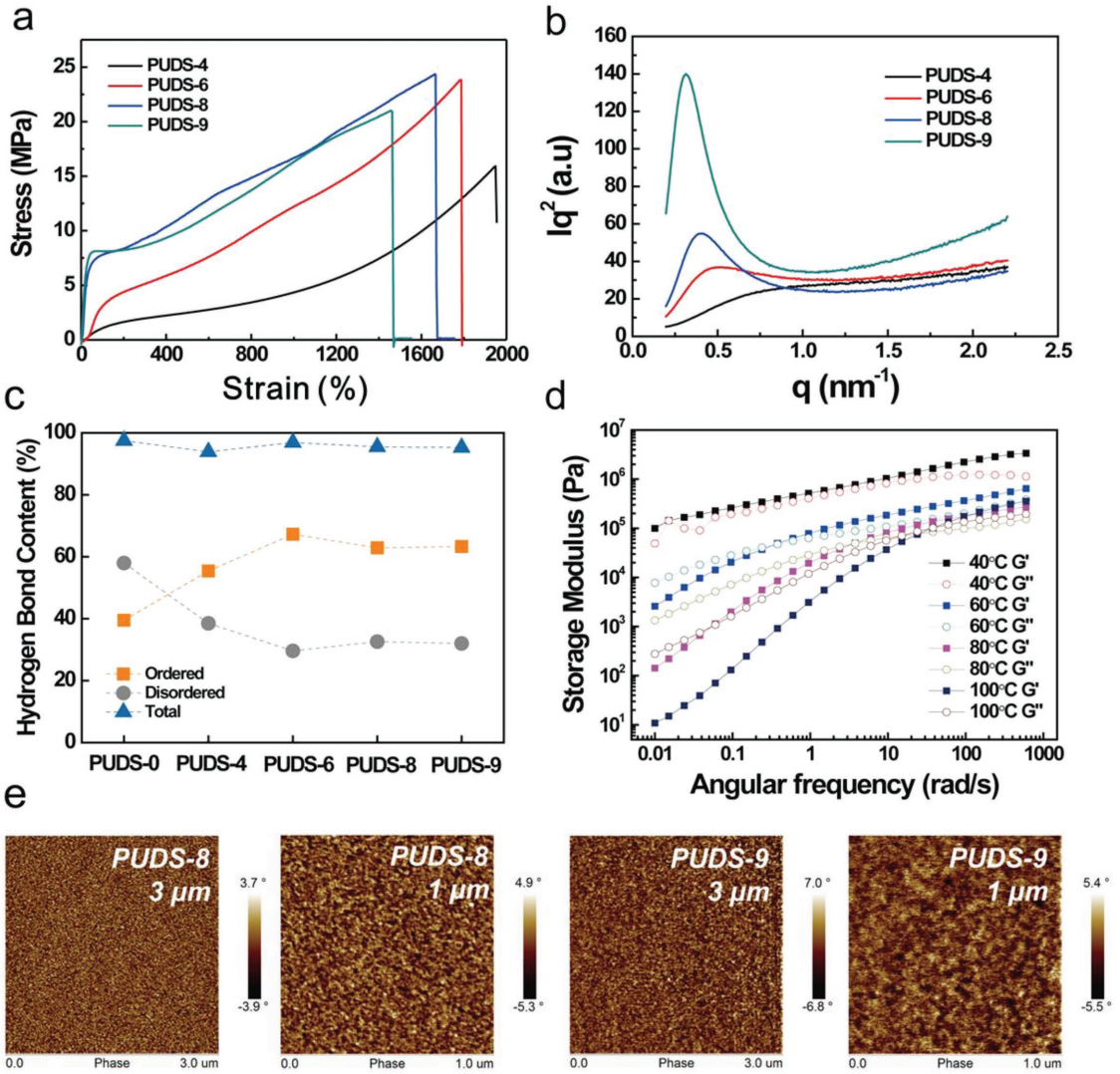


Figure 1. Characterization of the basic bulk mechanical properties and multiphase morphology of the PUDS elastomer. a) Typical strain–stress curves of the PUDS samples. b) Iq^2–q profiles of the PUDS samples. c) The content of the hydrogen bonds in the PUDS samples. d) Storage shear modulus G' and loss shear modulus G'' as functions of angular frequency ω for the PUDS-8 at different sweeping temperatures. e) AFM images of PUDS-8 and PUDS-9.

distinct aggregation of the hard segments and the increasing microphase domain size in the material. Notably, the strong hydrogen bonding in the hard segments provides a strong driving force for phase separation. Figure S4 (Supporting Information) shows the attribution of infrared spectra band for stretching vibration of C=O groups in TPU. The stretching vibration region of C=O groups is divided into three peaks. It is consistent with the literature,[19,20] except for some difference in the peak locations, which is related to the different types of isocyanate. The stretching vibration region of free hydrogen-bonded C=O groups appears at 1735 cm^{-1} and the ordered hydrogen-bonded C=O groups at 1695 cm^{-1} as well as the disordered hydrogen-bonded C=O groups at 1720 cm^{-1}. The FTIR spectra of the PUDS-4/6/8/9 samples were fitted using Gauss Lorenz curves and the percentage of the hydrogen bond content of all the samples are listed in Figure 1c. The PUDS systems have a high degree of hydrogen bonding (up to 95%). The hydrogen bond interaction in the system tends to be more ordered with the increase of the hard segment content. A higher degree of hydrogen bonding in the hard segments will induce a stronger phase separation of hard and soft segments in the systems.

The microphase separated structure of the self-healing PUDS systems was further verified by atomic force microscopy (AFM) (Figure 1e). The results show the aggregation of both the soft segments (dark areas) and hard segments (bright areas) clearly. Since the system is not crystallized, the microscale aggregation of the hard segments acts as the physical crosslinking and reinforcement of the TPU to enhance the mechanical properties. The soft segments in the soft phase act as the matrix of TPUs, enabling their high stretchability. The dynamic disulfide bonds in hard segments were located in the hard microphase. Therefore, below the T_g of the hard microphase, dynamic bonds can be locked due to the immobility of

© 2018 WILEY-VCH Verlag GmbH & Co. KGaA, Weinheim

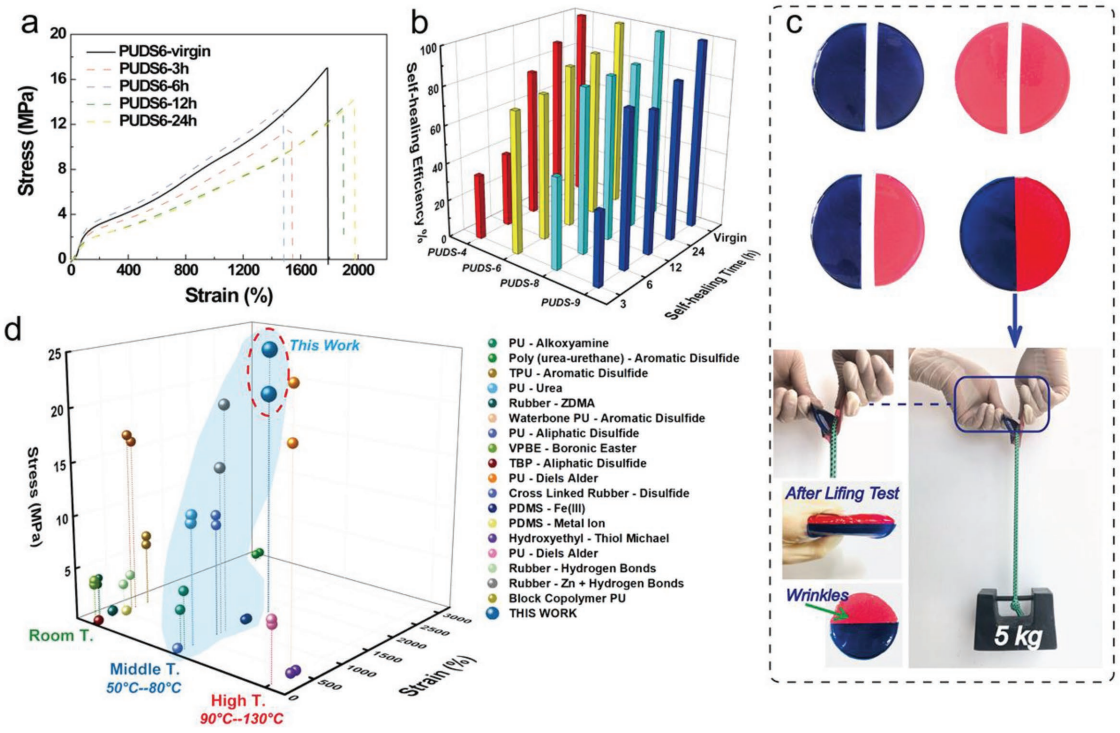


Figure 2. Self-healing tests of the PUDS bulk material samples. a) Comparison of the mechanical properties between virgin and full-cut PUDS samples at different self-healing time. b) The self-healing efficiency of completely fractured PUDS samples after different self-healing time. c) Images of the colored PUDS-6 film that was cut into two pieces, respectively, and healed for 4 h at 70 °C, and then subjected to a 5 kg weight lifting test. d) Comparison of the mechanical properties of the virgin and repaired samples reported in this work and those reported in related references.[5b–f,6c,d,7b,f,8a–c,9a,12,15–18] In each pair, the upper patterns represent the mechanical properties of the virgin samples, the lower patterns represent the mechanical properties of the self-healing samples.

chain. Upon external mechanical forces, the dynamic bonds, a weak part of the chain, were protected in the hard microphase allowing for excellent mechanical properties. We name this as "phase-locked" dynamic bonds.

As mentioned above, the multiblock polymer chain has dynamic disulfide linkages predominantly confined in the hard microphase, which is surrounded by the soft matrix. The dynamic bond exchange reaction enables stress relaxation and chain rearrangement in the materials after the activation of the glassy microphase by heating. The stress relaxation enabled by the dynamic exchange reaction was evaluated by rheological measurements via a frequency sweep test (Figure 1d). In the linear viscoelastic region, when the temperature is low, such as room temperature, the G' is much higher than G'', indicating the elastic response of the material. In addition, the stress relaxation time is very long, which can be attributed to two factors: first, the bond lifetime of the dynamic disulfide bonds is relatively long at low temperature; second, the hard microphase is in the viscoelastic state, which can partially immobilize the highly dynamic bonds. The obvious crossover point of G' and G'' appears at the sweep temperature over 60 °C, indicating that the disulfide exchange reaction occurs obviously in the system. Furthermore, the crossover point moves to the high-frequency direction with increasing sweeping temperature, implying that the disulfide exchange reaction is temperature dependent. The different frequencies (ω) at the crossover point at different temperatures indicates the relaxation time or bond lifetime ($1/\omega$) for disulfide bonds. The data were fitted with the Arrhenius equation (Figure S10, Supporting Information). The stress relaxation activation energy is calculated as 122 kJ mol^{-1}, which also reflects the activation energy of the dynamic reaction.[4d,21] The relatively high reaction activation energy indicates that the exchange reaction is sensitive to temperature. This feature is beneficial for this kind of high-strength self-healing elastomer. On the one hand, the long relaxation time near room temperature endows the materials with dimension stability and excellent mechanical properties. On the other hand, the low lifetime of the disulfide bonds at high temperatures provides the PUDS with efficient and robust healing capability.

To investigate the full-cut self-healing properties of the PUDS samples, dumbbell virgin samples (PUDS-4, PUDS-6, PUDS-8, and PUDS-9) were completely cut in half and then joined at 70 °C for different times. The results show that the PUDS samples possess high self-healing capability (typical tensile curves are shown in **Figure 2**a; the others are in Figure S11 and Table S4, Supporting Information). Healing efficiency (%) is defined as the ratio of the stress of healed and virgin materials. Different self-healing times result in different self-healing efficiencies of the PUDS samples (Figure 2b). The ultimate self-healing efficiency after complete fracture (after 24 h) of the four PUDS samples can reach approximately 85%. Among the four samples, the PUDS-6 sample seems to display the fastest self-healing speed, while the PUDS-8 sample can reach a higher level self-healing efficiency of up to 86.4% at 70 °C for 6 h. The self-healing ability of the PUDS

© 2018 WILEY-VCH Verlag GmbH & Co. KGaA, Weinheim

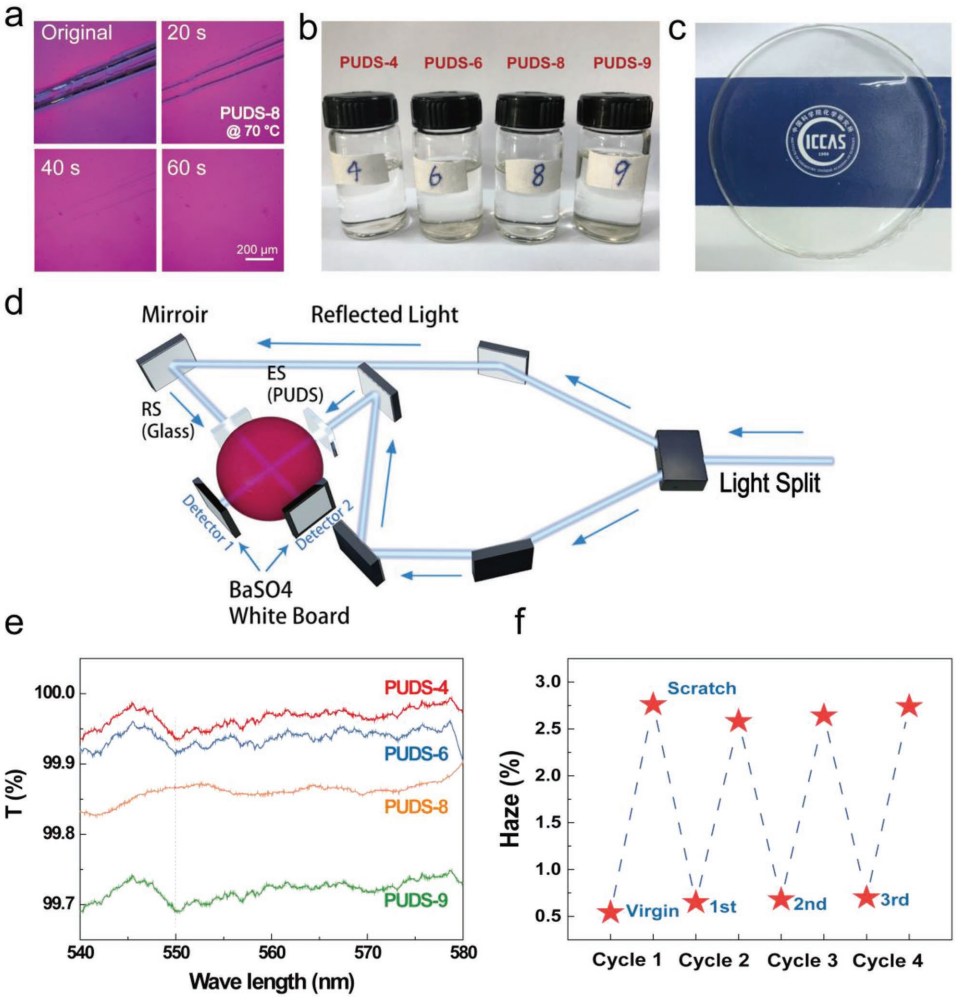


Figure 3. Self-healing tests of the PUDS films. a) Optical microscopy images of the scratch self-healing process. b) Series of PUDS samples synthesized: colorless transparent liquids. c) The transparent casting film of PUDS-8. d) An optical schematic diagram of the UV–vis spectrometer. e) Transmittance curves of the PUDS samples. f) Reversible changes in the haze value of PUDS-8 samples during scratching–self-healing cycles.

systems is believed to mainly depend on the disulfide content and the interaction of hydrogen bonds between different polymer chains. A higher disulfide content in a PUDS system indicates higher concentration of dynamic bonds on the crack surface to better re-bond the fracture area. Thus, the PUDS systems with higher disulfide contents should display an efficient self-healing ability. However, the self-healing efficiency is also affected by the ability to overcome self-healing barriers, i.e., the mobility of the free groups on the fracture surface, which is closely related to the hard and soft segment fractions. The higher the content of hard segments in the system is, the more hydrogen bonding interactions between the molecular chains are. The stronger hydrogen bonding interaction may depress the movement of the molecular chains, thus hindering the exchange of dynamic chemical bonds. Therefore, the good balance of the hard segment content and the disulfide bond content gives the best self-healing ability. In comparison to the related references reported to date (Figure 2d), the PUDS system designed in this work not only has a superior ultimate tensile stress and strain but also shows a better self-healing ability at a moderate temperature.

In order to visualize the excellent self-healing properties of the PUDS samples, the circular PUDS-8 film colored blue and red with 70.0 mm in diameter and a thickness of 1.5 mm was cut into two pieces, respectively, and healed any two color pieces at 70 °C for 4 h. The self-healed sample was able to lift 5 kg of weight without tearing (Figure 2c). After the lifting test, the healed sample was not damaged except for a few wrinkles on the surface (Figure 2c). Regarding the potential applications of the PUDS, scratch healing performance is another important property of the samples. **Figure 3**a shows that the scratches on the PUDS-8 film were observed to become increasingly shallow and finally faded away within 60 s upon heating at 70 °C. When the temperature increases above the T_g of the hard segment, the dynamic bonds are activated and dynamic exchange reactions begin to occur within the system. Meanwhile, as the PUDS sample is thermoplastic elastomer, the molecular chain shows enhanced mobility under heating. This speeds up the exchange of disulfide bonds to some extent, promoting the rapid scratch healing. We also used blades to create scratches on the surface of a control sample without dynamic bonds (PUDS-0)

© 2018 WILEY-VCH Verlag GmbH & Co. KGaA, Weinheim

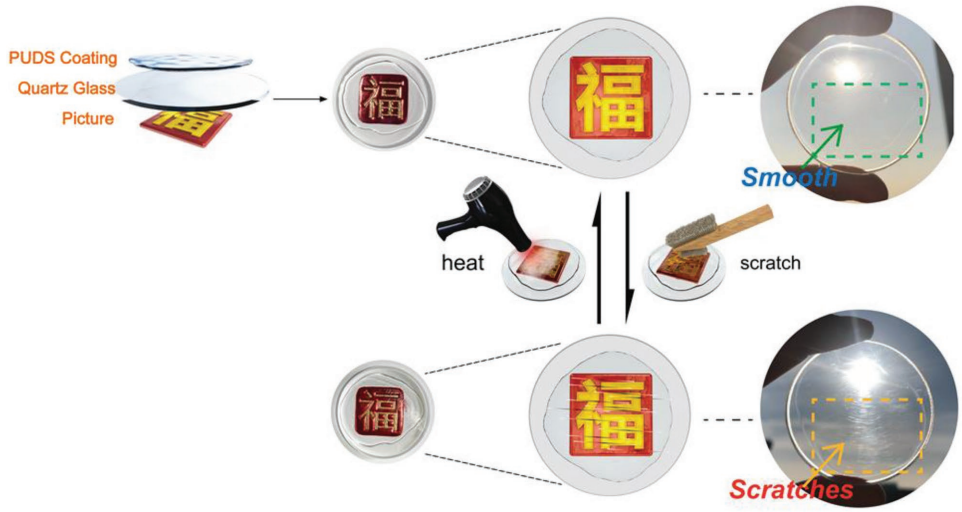


Figure 4. PUDS self-healing coating was self-healed by a heat gun after routine scratches (50–80 µm width) for optical lens protection applications.

and heated the scratched sample at 70 °C for 30 min. The scratch on the PUDS-0 sample was not repaired (Figure S12, Supporting Information). Besides, it can be seen from the frequency sweep test that the frequency corresponding to the crossover point of G' and G'' for PUDS-0 (Figure S9, Supporting Information) under the self-healing temperature (over 60 °C) is much lower than that of the samples containing disulfide bonds (PUDS-8, Figure 1d). This result indicates that the disulfide bond exchange reaction instead of thermal motion of molecular chains plays the critical role in rapid scratch self-healing of the system.

Because the system was amorphous and the soft segments and hard segments were phase separated into the nanoscale domains, the PUDS samples exhibit superior transparency while retaining their excellent mechanical properties and efficient self-healing performance. To evaluate the high transparency of the PUDS samples in the visible light region, a UV–vis spectrometer with an integrating sphere attachment was used as Figure 3d. The transmission spectra of the PUDS coatings with a thickness of 150 µm suggest that the transparency of the PUDS samples is equivalent to that of the regular glass at 550 nm (according to ASTM D1003, Figure 3e). With the increasing content of the hard segments in the system, the size of the hard segments domains increased (Figure 1e), and the transmittance of the samples decreased very little (PUDS-4: 99.93%, PUDS-6: 99.91%, PUDS-8: 99.87%, PUDS-9: 99.69%).

The PUDS sample can be utilizd as a self-healing coating. As the coatings may be scratched more than once for practical application, we simulated several cycles of scratch recovery test and evaluated the results based on the haze value (Equation S2, Supporting Information) of each state of the PUDS coating. A copper brush was used to create 50–80 µm wide scratches until the scratches covered the entire surface. Figure 3f shows the change in haze value during repeated scratching–self-healing. Compared with the virgin coating sample, the haze value of the scratched sample (approximately 2.6%) is much higher. By contrast, the haze value of the PUDS coating after several self-healing cycles was basically restored to its initial state (haze value = 0.6–0.7%). Therefore, the superior transparent PUDS coating achieves repeated scratch-healing without compromising its visible-light transmittance and haze.

Owing to its superior transparency and self-healing ability, the PUDS has a promising application as an optical lens coating that can repair itself after routine scratches. As a proof-of-concept demonstration, a typical application of this self-healing material was presented by preparing PUDS-8 coatings on the surface of the optical lens for repeated scratch healing with a heat gun. To prove the transparency of the coating and the even distribution of scratches on the coating surfaces, the Chinese character 福, which represents good luck and happiness, was placed under the optical lens (**Figure 4**). Originally, the transparency of the coatings resembles that of the optical lens. After the coatings were scraped with the copper brush, the haloes can be obviously observed under the sunlight due to light scattering. However, after self-healing, the haloes on the sample fade away and the surface of the sample becomes very smooth. The mechanical damage was fully recovered within 3 min with a heat gun (about 70 °C). In addition, the scratch healing of the protective coating can be repeated several times. After self-healing, the surface of the coating was still as smooth and transparent as before.

In summary, a novel colorless transparent and self-healing polyurethane system containing disulfide bonds was successfully synthesized in this work. The PUDS systems possess three distinct characteristics. First, comparing to the other self-healing polyurethane materials reported to-date, the self-healing PUDS systems with roboust mechanical properties simultaneously possess a maximum tensile stress of 25 MPa and a high strain of over 1600%. The second, the self-healing PUDS systems are all colorless and as highly transparent as quartz glass. The third, the scratches on the surface can be completely healed within 60 s, and the healing efficiency of the full-cut fractured PUDS samples tested reached over 85% within 6 h at 70 °C. The prominent properties are derived from the rational molecular design and microphase control. Excellent mechanical and healing properties are achieved by a novel concept of

© 2018 WILEY-VCH Verlag GmbH & Co. KGaA, Weinheim

"phase-locked dynamic bonds," where the highly dynamic chemical bonds protected by the viscoelastic hard microphase domains can be facilly locked and unlocked by temperature. The combination of using the aliphatic disulfide compounds and the alicyclic isocyanates with high steric hindrance allows for completely amorphous colorless transparent materials. The unique self-healing polyurethane system designed in this work finds great potential applications as protective films for precision optical lenses, flexible display screen, automobile, and aircraft lighting finishes. Moreover, the cost-effective, widely available resource and facile synthesis also make it possible for up-scale practical applications.

Experimental Section

Experimental details are given in the Supporting Information.

Supporting Information

Supporting Information is available from the Wiley Online Library or from the author.

Acknowledgements

Y.L. and X.K. contributed equally to this work. This work was financially supported by the National Natural Science Foundation of China (No. 21774135). The BL16B1 beamline of SSRF is acknowledged for kindly providing beam time and assistance.

Conflict of Interest

The authors declare no conflict of interest.

Keywords

disulfide, phase-locked design, polyurethane, rapid self-healing, transparency

Received: April 21, 2018
Revised: June 27, 2018
Published online:

[1] a) P. M. Imbesi, C. Fidge, J. E. Raymond, S. I. Cauët, K. L. Wooley, *ACS Macro Lett.* **2012**, *1*, 473; b) Y. Yang, M. W. Urban, *Chem. Soc. Rev.* **2013**, *42*, 7446; c) J. L. Mynar, T. Aida, *Nature* **2008**, *451*, 895.

[2] S. García, H. Fischer, S. van Der Zwaag, *Prog. Org. Coat.* **2011**, *72*, 211.

[3] a) Z. Wei, J. Yang, Z. Liu, F. Xu, J. Zhou, M. Zrínyi, Y. Osada, Y. Chen, *Adv. Funct. Mater.* **2015**, *25*, 1352; b) V. Yesilyurt, M. J. Webber, E. A. Appel, C. Godwin, R. Langer, D. G. Anderson, *Adv. Mater.* **2016**, *28*, 86.

[4] a) T.-P. Huynh, P. Sonar, H. Haick, *Adv. Mater.* **2017**, *29*, 1604973; b) B. C. Tee, C. Wang, R. Allen, Z. Bao, *Nat. Nanotechnol.* **2012**, *7*, 825; c) J. Y. Oh, S. Rondeau-Gagné, Y.-C. Chiu, A. Chortos, F. Lissel, G.-J. N. Wang, B. C. Schroeder, T. Kurosawa, J. Lopez, T. Katsumata, J. Xu, C. Zhu, X. Gu, W.-G. Bae, Y. Kim, L. Jin, J. W. Chung, J. B. H. Tok, Z. Bao, *Nature* **2016**, *539*, 411; d) J. Deng, X. Kuang, R. Liu, W. Ding, A. C. Wang, Y.-C. Lai, K. Dong, Z. Wen, Y. Wang, L. Wang, H. J. Qi, T. Zhang, *Adv. Mater.* **2018**, *30*, 1705918; e) J. Liu, C. Tan, Z. Yu, N. Li, C. Abell, O. A. Scherman, *Adv. Mater.* **2017**, *29*, 22.

[5] a) X. Liu, M. Zhong, F. Shi, H. Xu, X. Xie, *Chin. J. Polym. Sci.* **2017**, *35*, 1253; b) X. Jia, J. Mei, J. Lai, C. Li, X. You, *Macromol. Rapid Commun.* **2016**, *37*, 952; c) L. Liu, S. Liang, Y. Huang, C. Hua, J. Yang, *Chem. Commun.* **2017**, *53*, 12088; d) P. Cordier, F. Tournilhac, C. S. Ziakovic, L. Leibler, *Nature* **2008**, *451*, 977; e) J. Liu, J. Liu, S. Wang, J. Huang, S. Wu, Z. Tang, B. Guo, L. Zhang, *J. Mater. Chem. A* **2017**, *5*, 25660; f) S. Yoshida, H. Ejima, N. Yoshie, *Adv. Funct. Mater.* **2017**, *27*, 1701670; g) A. Das, A. Sallat, F. Böhme, M. Suckow, D. Basu, S. Wießner, K. W. Stöckelhuber, B. Voit, G. Heinrich, *ACS Appl. Mater. Interfaces* **2015**, *7*, 20623; h) Y. Wang, X. Liu, S. Li, T. Li, Y. Song, Z. Li, W. Zhang, J. Sun, *ACS Appl. Mater. Interfaces* **2017**, *9*, 29120; i) N. Chen, L. Qin, Q. Pan, *J. Mater. Chem. A* **2018**, *6*, 6667; j) X. Kuang, K. Chen, C. K. Dunn, J. Wu, V. C. F. Li, H. J. Qi, *ACS Appl. Mater. Interfaces* **2018**, *10*, 7381.

[6] a) X. Kuang, G. Liu, X. Dong, D. Wang, *Macromol. Mater. Eng.* **2016**, *301*, 535; b) S. Yu, R. Zhang, Q. Wu, T. Chen, P. Sun, A*dv. Mater.* **2013**, *25*, 4912; c) P. Du, X. Liu, Z. Zheng, X. Wang, T. Joncheray, Y. Zhang, *RSC Adv.* **2013**, *3*, 15475; d) C. Yuan, M. Rong, M. Zhang, *Polymer* **2014**, *55*, 1782; e) X. Kuang, G. Liu, X. Dong, D. Wang, *Polymer* **2016**, *84*, 1; f) R. Göstal, S. Hecht, *Angew. Chem., Int. Ed.* **2014**, *53*, 8784; g) Z. Zhang, M. Rong, M. Zhang, *Adv. Funct. Mater.* **2018**, *28*, 1706050; h) H. Xiang, M. Rong, M. Zhang, *Polymer* **2017**, *108*, 339.

[7] a) I. Azcune, I. Odriozola, *Eur. Polym. J.* **2016**, *84*, 147; b) Z. Lei, H. Xiang, Y. Yuan, M. Rong, M. Zhang, *Chem. Mater.* **2014**, *26*, 2038; c) J. M. Matxain, J. M. Asua, F. Ruipérez, *Phys. Chem. Chem. Phys.* **2016**, *18*, 1758; d) L. Imbernon, E. K. Oikonomou, S. Norvez, L. Leibler, *Polym. Chem.* **2015**, *6*, 4271; e) T. Wan, D. Chen, *J. Mater. Sci.* **2017**, *52*, 197; f) A. Rekondo, R. Martin, A. R. Luzuriaga, G. Cabañero, H. J. Grande, I. Odriozola, *Mater. Horiz.* **2014**, *1*, 237; g) Y. Lu, Z. Guan, *J. Am. Chem. Soc.* **2012**, *134*, 14226; h) N. Kuhl, S. Bode, R. K. Bose, J. Vitz, A. Seifert, S. Hoeppener, S. J. Garcia, S. Spange, S. van der Zwaag, M. D. Hager, U. S. Schubert, *Adv. Funct. Mater.* **2015**, *25*, 3295.

[8] a) B. Zhang, Z. A. Digby, J. A. Flum, P. Chakma, J. M. Saul, J. L. Sparks, D. Konkolewicz, *Macromolecules* **2016**, *49*, 6871; b) J. J. Cash, T. Kubo, A. P. Bapat, B. S. Sumerlin, *Macromolecules* **2015**, *48*, 2098; c) G. Fu, L. Yuan, G. Liang, A. Gu, *J. Mater. Chem. A* **2016**, *4*, 4232; d) X. An, R. H. Aguirresarobe, L. Irusta, F. Ruipérez, J. M. Matxain, X. Pan, N. Aramburu, D. Mecerreyes, H. Sardon, J. Zhu, *Polym. Chem.* **2017**, *23*, 3641; e) L. Yang, Y. Lin, L. Wang, A. Zhang, *Polym. Chem.* **2014**, *5*, 153; f) J. Chen, L. Fang, Z. Xu, C. Lu, *Prog. Org. Coat.* **2016**, *101*, 543; g) Z. Zhang, M. Rong, M. Zhang, *Polymer* **2014**, *55*, 3936; h) C. Yuan, M. Rong, M. Zhang, Z. Zhang, Y. Yuan, *Chem. Mater.* **2011**, *23*, 5076.

[9] a) J. Canadell, H. Goossens, B. Klumperman, *Macromolecules* **2011**, *44*, 2536; b) U. Lafont, H. van Zeijl, S. van der Zwaag, *ACS Appl. Mater. Interfaces* **2012**, *4*, 6280; c) J. Jiang, B. Qi, M. Lepage, Y. Zhao, *Macromolecules* **2007**, *40*, 790; d) S. Ji, W. Cao, Y. Yu, H. Xu, *Angew. Chem., Int. Ed.* **2014**, *53*, 6781; e) Y. Amamoto, H. Otsuka, A. Takahara, K. Matyjaszewski, *Adv. Mater.* **2012**, *24*, 3975; f) H. Otsuka, S. Nagano, Y. Kobashi, T. Maeda, T. Takahara, *Chem. Commun.* **2010**, *46*, 1150; g) J. Ling, M. Rong, M. Zhang, *Chin. J. Polym. Sci.* **2014**, *32*, 1286.

[10] a) A. Ruiz de Luzuriaga, R. Martin, N. Markaide, A. Rekondo, G. Cabanero, J. Rodriguez, I. Odriozola, *Mater. Horiz.* **2016**, *3*, 241; b) L. Zhang, L. Chen, S. J. Rowan, *Macromol. Chem. Phys.* **2017**, *218*, 1600320.

© 2018 WILEY-VCH Verlag GmbH & Co. KGaA, Weinheim

[11] R. Martin, A. Rekondo, A. R. de Luzuriaga, G. Cabañero, H. J. Grande, I. Odriozola, *J. Mater. Chem. A* **2014**, *2*, 5710.
[12] S. Kim, H. Jeon, S. Shin, S. Park, J. Jegal, S. Hwang, D. X. Oh, J. Park, *Adv. Mater.* **2017**, *30*, 1705145.
[13] H.-W. Engels, H.-G. Pirkl, R. Albers, R. W. Albach, J. Krause, A. Hoffmann, H. Casselmann, J. Dormish, *Angew. Chem., Int. Ed.* **2013**, *52*, 9422.
[14] Y. Berezkin, M. Urick, in *Polymers for Personal Care and Cosmetics*, American Chemical Society, Washington, DC, USA **2013**.
[15] Y. Kim, P. H. Huh, B. K. Kim, *J. Polym. Sci. Part B: Polym. Phys.* **2015**, *53*, 468.
[16] C. Xu, L. Cao, B. Lin, X. Liang, Y. Chen, *ACS Appl. Mater. Interfaces* **2016**, *8*, 17728.
[17] R. H. Aguirresarobe, L. Martin, M. J. Fernandez-Berridi, L. Irusta, *eXPRESS Polym. Lett.* **2017**, *11*, 266.
[18] Y. Xu, D. Chen, *Macromol. Chem. Phys.* **2016**, *217*, 1191.
[19] M. M. Coleman, D. J. Skrovanek, J. Hu, P. C. Painter, *Macromolecules* **1988**, *21*, 59.
[20] M. M. Coleman, K. H. Lee, D. J. Skrovanek, P. C. Painter, *Macromolecules* **1986**, *19*, 2149.
[21] X. Kuang, G. Liu, X. Dong, D. Wang, *Mater. Chem. Front.* **2016**, *1*, 111.

 © 2018 WILEY-VCH Verlag GmbH & Co. KGaA, Weinheim